Density functional theory of magnetic dipolar interactions

Camilla Pellegrini [1], Tristan Müller,[2] John K. Dewhurst,[2] Sangeeta Sharma,[3] Antonio Sanna [2], and Eberhard K. U. Gross[1]

[1]*Institute of Chemistry, Fritz Haber Center for Molecular Dynamics, The Hebrew University of Jerusalem, Jerusalem 91904, Israel*

[2]*Max-Planck-Institut für Mikrostrukturphysik, Weinberg 2, D-06120 Halle, Germany*

[3]*Max-Born-Institut für Nichtlineare Optik und Kurzzeitspektroskopie, Max-Born-Straße 2A, 12489 Berlin, Germany*

We propose a way to include magnetic dipole-dipole interactions in density functional theory calculations. To this end, we derive an approximation to the exchange-correlation energy functional associated with the spin-spin correction to the Coulomb force in the Breit-Pauli Hamiltonian. The local spin-density approximation is shown to be identically zero. First order nonlocal corrections are evaluated analytically within linear response to a noncollinear external magnetic field. The functional obtained is based on the exact-exchange energy of the magnetic electron gas with dipolar interactions and is estimated to be relevant at interatomic distances, or in the low electron density limit, where it amounts to one quarter of the magnetostatic energy. We expect our functional to improve over the current description of ground-state properties of inhomogeneous magnetic structures at the nanoscale and dipolar spin systems.

I. INTRODUCTION

The need for higher density data storage and practical schemes to implement quantum information processing [1–4] has led, in the last decades, to thriving research on non-conventional magnetic systems [5]. These include ultracold dipolar gases in optical lattices [6,7], low-dimensional or frustrated magnets [8], nanostructured magnetic materials [9], and molecular magnets [10]. All these systems show a complex magnetic behavior at the atomic scale, which results from the delicate interplay between Heisenberg exchange interactions and (tunable) spin-orbit coupling and dipolar interactions. In particular, new effects from the last, due to their long-range and anisotropic nature, are attracting great interest. While the picture of magnetic dipole-dipole interactions as a small classical perturbation might be enough to understand traditional magnetism, it seems to be no longer sufficient for the description of spin systems with strong magnetic moments and length scales approaching the nanometer range.

Currently, the most common and feasible approach to describe the magnetic behavior of a given material is the micromagnetic approach [11], which ignores the atomic structure of matter, neglects quantum effects, and uses classical physics in a continuum description of the system. Essentially, the atomic magnetic moments are assumed to vary slowly within a mesoscopic volume of the sample, so to define a mesoscopic average magnetization $\mathbf{M}(\mathbf{r})$. The magnetic Gibbs energy, which is the sum of four major contributions, i.e., exchange, magnetocrystalline anisotropy, Zeeman and dipolar energy, is formulated in terms of the continuous magnetization vector field and minimized to determine static magnetization structures. Specifically, the dipolar energy is derived from simplified magnetostatic Maxwell's equations and computed in terms of effective magnetic volume charges $\rho(\mathbf{r}) = -\nabla \cdot \mathbf{M}(\mathbf{r})$ and effective magnetic surface charges $\sigma(\mathbf{r}) = \mathbf{M}(\mathbf{r}) \cdot \mathbf{n}$

as

$$E_{\text{magstat}} = \frac{\mu_0}{2} \int_V \rho(\mathbf{r}) U(\mathbf{r}) d^3r + \frac{\mu_0}{2} \int_S \sigma(\mathbf{r}) U(\mathbf{r}) dS. \quad (1)$$

Here, the magnetic scalar potential $U(\mathbf{r})$ is the solution of the Poisson's equation $\Delta U(\mathbf{r}) = -\rho(\mathbf{r})$, i.e., has the general form

$$U(\mathbf{r}) = \frac{1}{4\pi} \int_V \frac{\rho(\mathbf{r}')}{|\mathbf{r} - \mathbf{r}'|} d^3r' + \frac{1}{4\pi} \int_S \frac{\sigma(\mathbf{r}')}{|\mathbf{r} - \mathbf{r}'|} dS'. \quad (2)$$

As is clear from Eqs. (1) and (2), the magnetostatic energy arises from inhomogeneities of the average magnetization $\mathbf{M}(\mathbf{r})$ on a mesoscopic scale. Micromagnetic simulations have proven to be generally a very reliable tool for investigating the properties of ferromagnetic nanostructures. However, due to the rapid advances in the synthesis of nanostructured materials, the continuum assumption behind these algorithms might be unjustified. E.g., highly inhomogeneous magnetic structures, laser-induced magnetization dynamics, and sample sizes approaching the atomic scale are a few cases that challenge the limits of micromagnetic theory and demand extensions to the standard approach.

On the other hand, the calculation of atomic properties and interactions at the quantum mechanical level is the realm of *ab initio* methods, such as density functional theory [12–14]. Density functional calculations of magnetic systems are mostly based on (nonrelativistic) spin-density functional theory (SDFT) [15]. Within SDFT, the dominant source of magnetic coupling is exchange, which originates from the Pauli exclusion principle and favors spin alignment (ferromagnetism). By minimizing the total energy functional, single-particle Kohn-Sham (KS) equations [16] are derived and solved self-consistently to determine the values of the charge density and the magnetization density. The applicability of the method depends crucially on physically sound

and numerically feasible approximations to the exchange-correlation (xc) part of the energy functional, which includes all quantum and many-body effects. The rotational invariance with respect to the spin quantization axis is broken by relativistic corrections to the Hamiltonian, i.e., dipole-dipole interaction and spin-orbit coupling. Both are of the same order $(1/c^2)$ in the weakly relativistic expansion of the full Lagrangian of quantum electrodynamics [17]. Spin-orbit effects, which are responsible for magnetocrystalline anisotropy, are often taken into account in practice by using nonrelativistic SDFT functionals together with Dirac- or Pauli-type KS equations. However, magnetic dipole-dipole interactions are currently not included in the formalism. SDFT calculations in the local spin-density approximation (LSDA) and beyond, have proven over the years to yield reliable results for large classes of magnetic materials, with collinear and noncollinear spin alignment. Nevertheless, based on the recent experimental advances, we propose in this paper a density functional treatment of the dipolar interaction as a pairwise interaction, with associated quantum effects.

We start with the weakly relativistic Hamiltonian

$$\hat{H} = \hat{T} + \int d^3r \{\hat{n}(\mathbf{r})v_{\text{ext}}(\mathbf{r}) + \mu_B \hat{\mathbf{m}}(\mathbf{r}) \cdot \mathbf{B}_{\text{ext}}(\mathbf{r})\}$$
$$+ \frac{e^2}{2} \int d^3r \int d^3r' \frac{\hat{n}(\mathbf{r})\hat{n}(\mathbf{r}')}{|\mathbf{r} - \mathbf{r}'|} + \hat{H}^{SS}, \quad (3)$$

which includes, beyond the usual Hamiltonian of spin-density functional theory, the mutual $1/c^2$ interaction $\hat{H}^{SS}$ between the spin magnetic moments of the electrons [18]. This term has the form [17,19]:

$$\hat{H}^{SS} = -2\pi\mu_B^2 \int d^3r \int d^3r' \, \hat{\mathbf{m}}^i(\mathbf{r})\delta_{ij}^{\perp}(\mathbf{r} - \mathbf{r}')\hat{\mathbf{m}}^j(\mathbf{r}'),$$
$$(4a)$$

$$\delta_{ij}^{\perp}(\mathbf{r} - \mathbf{r}') = \frac{2}{3}\delta_{ij}\delta(\mathbf{r} - \mathbf{r}') + d_{ij}(\mathbf{r} - \mathbf{r}'), \quad (4b)$$

representing the interaction $-\frac{\mu_B^2}{2}\int d^3r \, \hat{\mathbf{m}}(\mathbf{r}) \cdot \hat{\mathbf{B}}(\mathbf{r})$ of the magnetization density $\hat{\mathbf{m}}(\mathbf{r})$ with the magnetic induction $\hat{\mathbf{B}}_i(\mathbf{r}) = 4\pi \int d^3r'\delta_{ij}^{\perp}(\mathbf{r} - \mathbf{r}')\hat{\mathbf{m}}^j(\mathbf{r}')$ generated by the magnetization distribution within the sample. Here, the magnetization density operator is defined as $\hat{\mathbf{m}}(\mathbf{r}) = \hat{\psi}^{\dagger}(\mathbf{r})\sigma\hat{\psi}(\mathbf{r})$, where $\hat{\psi}(\mathbf{r})$, $\hat{\psi}^{\dagger}(\mathbf{r})$ are the usual Pauli spinor field operators and σ is the vector of Pauli matrices. $\delta^{\perp}$ denotes the transverse delta function [20,21], $\mu_B = e\hbar/(2m_ec)$ is the Bohr magneton. Repeated indices are assumed to be summed over. As one can see, Eq. (4a) is the sum of two contributions. The first contribution, coming from the first term of Eq. (4b),

$$\hat{H}^{SC} = -\frac{4\pi\mu_B^2}{3}\int d^3r \, \hat{\mathbf{m}}(\mathbf{r}) \cdot \hat{\mathbf{m}}(\mathbf{r}), \quad (5)$$

is a contact interaction, which depends on the magnetization density at the same point. This is the counterpart of the Fermi contact interaction between an electron and a nucleus. The second contribution, coming from the second term of Eq. (4b),

$$\hat{H}^{\text{dip}} = -2\pi\mu_B^2 \int d^3r \int d^3r' \, \hat{\mathbf{m}}^i(\mathbf{r})d_{ij}(\mathbf{r} - \mathbf{r}')\hat{\mathbf{m}}^j(\mathbf{r}'), \quad (6)$$

represents the dipolar interaction between two spin densities. Here, the tensor d_{ij} is defined as follows

$$d_{ij}(\mathbf{r} - \mathbf{r}') \equiv -\frac{1}{4\pi}\nabla_i\nabla_j'\frac{1}{|\mathbf{r} - \mathbf{r}'|} + \frac{1}{3}\delta_{ij}\delta(\mathbf{r} - \mathbf{r}')$$
$$= \frac{1}{4\pi R^3}(3\bar{R}_i\bar{R}_j - \delta_{ij}), \quad (7)$$

where $\mathbf{R} = \mathbf{r} - \mathbf{r}'$ is the relative position of the electrons, and $\bar{\mathbf{R}}$ denotes the unit vector along $\mathbf{R}$. The expression for d_{ij} is understood to be regularized at $R = 0$ [19,21]. Physically, Eq. (6) together with Eq. (7) describe the interaction between the magnetization density at $\mathbf{r}$ and the dipolar field created by the magnetization distribution at all the other points $\mathbf{r}' \neq \mathbf{r}$. Nevertheless, the contact term δ_{ij} in Eq. (7) is included to ensure that the diagonal elements of d_{ij} satisfy the Laplace equation $\Delta(1/|\mathbf{r} - \mathbf{r}'|) = -4\pi\delta(\mathbf{r} - \mathbf{r}')$ for the scalar potential generated by the magnetic charge density in the system. The dipolar tensor, as defined by Eq. (7), is both traceless and symmetric.

The present paper is organized as follows: In Sec. II A we point out the equivalence between the magnetostatic energy contribution implemented in the micromagnetic approach and the classical Hartree term of SDFT for the dipolar interaction. The SDFT framework then naturally leads to the inclusion of a dipolar xc functional to account for quantum effects. In Sec. II B we address the adequacy of a LSDA for the dipolar xc energy. In Sec. II C we derive a nonlocal and noncollinear exchange energy functional as leading order quantum correction to the magnetostatic energy. In Sec. III we briefly consider the density functional treatment of the spin contact interaction of Eq. (4b).

II. DIPOLE-DIPOLE INTERACTION FUNCTIONAL

A. Hartree energy functional

The Hartree term for the magnetic dipole-dipole interaction has been derived by Jansen [22] in a broader analysis of magnetic anisotropy contributions within the framework of density functional theory. The dipolar energy in the Hartree approximation is obtained by simply replacing the magnetization density operator $\hat{\mathbf{m}}(\mathbf{r})$ in Eqs. (6) and (7) by the expectation value $\mathbf{m}(\mathbf{r})$:

$$E_H^{\text{dip}}[\mathbf{m}] = -\frac{\mu_B^2}{2}\int d^3r \int d^3r'$$
$$\times \frac{3(\mathbf{m}(\mathbf{r}) \cdot \bar{\mathbf{R}})(\mathbf{m}(\mathbf{r}') \cdot \bar{\mathbf{R}}) - \mathbf{m}(\mathbf{r}) \cdot \mathbf{m}(\mathbf{r}')}{R^3}. \quad (8)$$

The Hartree method, in which the dipolar interaction is taken into account by a mean field type of approximation, is qualitatively equivalent to the micromagnetic approach. [Formally, this can be seen by rewriting Eq. (1) as $E_{\text{magstat}} = -\frac{\mu_0}{2}\int d^3r \int d^3r' \mathbf{M}(\mathbf{r}) \cdot \mathbf{N}(\mathbf{r} - \mathbf{r}') \cdot \mathbf{M}(\mathbf{r}')$, where the demagnetizing tensor for a ferromagnetic body of arbitrary shape is given by $\mathbf{N}(\mathbf{r} - \mathbf{r}') = -\frac{1}{4\pi}\nabla\nabla'(1/|\mathbf{r} - \mathbf{r}'|)$.] Differences in the dipolar energy calculated from Eq. (8) and from the micromagnetic formula (1) are due to deviations of the actual atomic distribution $\mathbf{m}(\mathbf{r})$ from its average $\mathbf{M}(\mathbf{r})$ over a mesoscopic cell of atomic volumes. We emphasize that, so far, only this mean field contribution to the dipolar energy
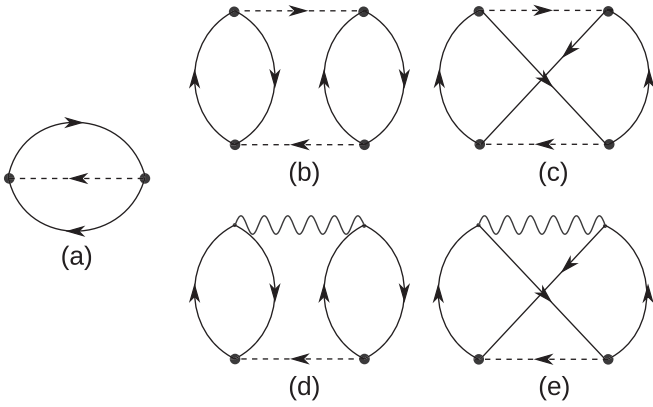
FIG. 1. Diagrammatic expansion of the exchange-correlation energy of the homogeneous electron gas with dipolar spin-spin interactions, up to second order. (a) Exchange energy diagram. (b),(d) Direct and (c),(e) exchange diagrams contributing in second order to the correlation energy. Dashed lines indicate dipolar interactions; wiggly lines indicate Coulomb interactions.

has been implemented in actual calculations of magnetic structures. However, the Hartree treatment of a pairwise interaction is usually a crude approximation (see, e.g., the case of the Coulomb interaction), as it completely neglects quantum many-body effects and is affected by a self-interaction error. In the next sections we discuss how to derive an improved estimate of the real dipolar energy by adding, as a natural step of the SDFT formalism, an approximate exchange-correlation term.

B. LSDA

The approximation to the exchange (x) energy functional most widely used in SDFT is the local spin-density approximation [15]. In LSDA, the x energy of a nonuniform magnetic system is approximated at each point by the x energy of the homogeneous electron gas (HEG) with the same spin density as the local density. Choosing a coordinate system with the z axis along the direction of the local spin, the x energy density of the spin polarized nonrelativistic HEG with dipolar interactions [see diagram (a) of Fig. 1] can be evaluated as

$$e_x^{\text{dip}}(\mathbf{r}) = \frac{\mu_B^2}{2} \int d^3r' \rho_{\alpha\beta}(\mathbf{R})\sigma_{\nu\alpha}^i d_{ij}(\mathbf{R})\sigma_{\beta\mu}^j \rho_{\mu\nu}(-\mathbf{R}), \quad (9)$$

where $\rho_{\alpha\beta}(\mathbf{R}) = \int d^3k \, \psi_{\mathbf{k}\sigma}^\dagger(\mathbf{r}\alpha)\psi_{\mathbf{k}\sigma}(\mathbf{r}'\beta)$ is the one-body density matrix with spin orbitals $\psi_{\mathbf{k}\sigma}(\mathbf{r}\alpha) = 1/\sqrt{V}e^{i\mathbf{k}\cdot\mathbf{r}}\delta_{\sigma\alpha}$. Since the HEG is spherically symmetric, the density matrix depends only on the modulus of the distance, i.e., $\rho(\mathbf{R}) = \rho(R)$. It is then easy to show that Eq. (9) gives a null contribution, as one essentially integrates a spherical harmonic with $l = 2$ and $m = 0$ over all angles. We thereby conclude that for the HEG, regardless of the spin polarization, the leading relativistic correction to the energy due to the dipole-dipole interaction vanishes. We point out that this is a general property of the interaction, and the obtained result is not affected by employing Dirac spinors for the electron field operators.
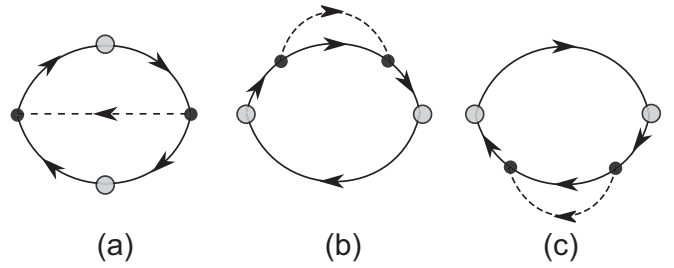

FIG. 2. First order Feynman diagrams for the spin density response function with magnetic dipole-dipole interaction (dashed line). The gray dots represent the external magnetic fields.

Nevertheless, the correlation energy of the dipolar HEG turns out to be finite. In second order it arises entirely from diagram (b) of Fig. 1, which readily translates into the Møller-Plesset (MP2) correlation energy per electron

$$E_c^{\text{(MP2)dip}} = -\frac{e^4\hbar^2k_F^4}{2m_e^3c^4\pi^2}\frac{43 - 46\ln 2}{525}. \quad (10)$$

For the same reason discussed above, in fact, diagram (c) vanishes, and it can be proven, in general, that all the diagrams involving one single dipole interaction line [thus including also diagrams (d) and (e) of Fig. 1], do not contribute to the energy.

C. Nonlocal exchange energy functional

We proceed to derive nonlocal corrections to the LSDA for the dipolar x energy functional. Corrections to the standard LSDA in SDFT are systematically constructed from the weakly inhomogeneous electron gas via the gradient expansion and the linear response. Here, we follow the second strategy, which allows one to account for small variations of $\mathbf{m}(\mathbf{r})$ at any $\mathbf{r}$. We thus consider the (spin-unpolarized) dipolar HEG subject to a weak external magnetic field $\delta V_{\mathbf{q}}^j(\mathbf{r}) \propto e^{i\mathbf{q}\cdot\mathbf{r}}\sigma^j$, which perturbs the magnetization density from the average value $\mathbf{m}_j$ to $\mathbf{m}_j + \delta\mathbf{m}_j(\mathbf{r})$. The wave vector $\mathbf{q}$ is assumed to be arbitrary, so that the approach is fully noncollinear. By expanding the dipolar x energy to second order in the deviation from the homogeneous limit, we have [14,23–25]

$$E_x^{\text{dip}}[\mathbf{m}] = \frac{\mu_B^2}{2} \int \frac{d^3q}{(2\pi)^3}K_x^{ij}(\mathbf{q})\delta m_i(\mathbf{q})\delta m_j(-\mathbf{q}), \quad (11)$$

where $\delta m_i(\mathbf{q})$ is the induced magnetization density variation (to be obtained from an actual calculation), and the x kernel is given by

$$K_x^{ij}(\mathbf{q}) \equiv \frac{\partial^2 E_x^{\text{dip}}}{\partial \mathbf{m}_i(\boldsymbol{q})\partial\mathbf{m}_j(-\boldsymbol{q})} = \frac{g_{kl}(\mathbf{q})}{\chi_0^{ik}(q)\chi_0^{jl}(q)}. \quad (12)$$

Here, K_x^{ij} is expressed in terms of the Lindhard response function of the HEG $\chi_0^{ik} = \partial m_i/\partial V_k$ and the linear response contribution to the dipolar x energy functional $g_{kl}(\mathbf{q}) \equiv \partial^2 E_x^{\text{dip}}/\partial V_{\mathbf{q}}^k \partial V_{-\mathbf{q}}^l$. The latter is represented diagrammatically in Fig. 2. Here, the vertex correction diagram (a) corresponds

to the analytic expression

$$g^{lk}(\mathbf{q}, 0) = \frac{2\pi}{\beta^2} \sum_{n,m} \int \frac{d^3k}{(2\pi)^3} \int \frac{d^3k'}{(2\pi)^3} v^{ij}_{\mathbf{k}-\mathbf{k}'} \sigma^i_{\alpha\delta} G^0_{\delta\epsilon}(k, i\epsilon_n) \sigma^l_{\epsilon\eta} G^0_{\eta\gamma}(|\mathbf{k}+\mathbf{q}|, i\epsilon_n) \sigma^j_{\gamma\beta} G^0_{\beta\zeta}(|\mathbf{k}'+\mathbf{q}|, i\epsilon'_m) \sigma^k_{\zeta\theta} G^0_{\theta\alpha}(k', i\epsilon'_m), \quad (13)$$

where $v^{ij}_{\mathbf{k}} = (\delta_{ij} - 3\bar{\mathbf{k}}_i\bar{\mathbf{k}}_j)/3$ is the Fourier transform [19] of the dipolar tensor of Eq. (7), and $G^0_{\alpha\beta}(k, i\omega_n) = \delta_{\alpha\beta}/(i\omega_n - \varepsilon_{\mathbf{k}})$ is the unperturbed Matsubara Green's function for the paramagnetic electron gas. Summing over the spin indices in Eq. (13) gives

$$Tr\{\sigma^i\sigma^l\sigma^j\sigma^k\} = 4\delta_{il}\delta_{jk}. \quad (14)$$

From Eq. (14), since the HEG is isotropic, we observe that Eq. (13) can be written in the following form

$$g^{ij}(\mathbf{q}, 0) = f(q)(\delta_{ij} - 3\bar{\mathbf{q}}_i\bar{\mathbf{q}}_j), \quad (15)$$

where $f(q)$ denotes a function of the modulus of $\mathbf{q}$ only, and the angular dependence of g on the indices of $\mathbf{q}$ is through the traceless and symmetric interaction tensor $v^{ij}_{\mathbf{k}-\mathbf{k}'}$. By assuming $\mathbf{q}$ in the direction of the z axis, i.e., $\mathbf{q} = q\bar{\mathbf{z}}$, we evaluate the function $f(q) = -g^{zz}(q\bar{\mathbf{z}})/2$ (note that one also has $g^{xx} = g^{yy} = -1/2\,g^{zz}$). Summing over the Matsubara frequencies gives

$$f(q) = \frac{8\pi}{3} \int \frac{d^3k}{(2\pi)^3} \left(\frac{n_{\mathbf{k}} - n_{\mathbf{k}+\mathbf{q}}}{\varepsilon_{\mathbf{k}} - \varepsilon_{\mathbf{k}+\mathbf{q}}}\right) \int \frac{d^3k'}{(2\pi)^3} \left(\frac{n_{\mathbf{k}'} - n_{\mathbf{k}'+\mathbf{q}}}{\varepsilon_{\mathbf{k}'} - \varepsilon_{\mathbf{k}'+\mathbf{q}}}\right) P_2(\cos\theta_{\mathbf{k}-\mathbf{k}'}), \quad (16)$$

where $n_{\mathbf{k}}$ is the Fermi distribution function and $P_2(\cos\theta_{\mathbf{k}}) = 1/2(3\cos^2\theta_{\mathbf{k}} - 1)$ is the Legendre polynomial of second order with $\cos\theta_{\mathbf{k}} = \bar{\mathbf{k}} \cdot \bar{\mathbf{z}}$. The main result of this paper is the exact evaluation of Eq. (16) in terms of one quadrature. We notice that by means of the transformations $\mathbf{k}^{(')} \to \pm\mathbf{k}^{(')} - \mathbf{q}/2$, it is possible to recast the $\sim \cos^2\theta_{\mathbf{k}-\mathbf{k}'}$ term of Eq. (16) in the form

$$I(q) = \frac{m_e^2}{8\pi^5\hbar^4 q^2} \int d^3k \int d^3k' \frac{n_{\mathbf{k}-\mathbf{q}/2} n_{\mathbf{k}'-\mathbf{q}/2}}{(\mathbf{k} \cdot \mathbf{q})(\mathbf{k}' \cdot \mathbf{q})} \left\{\left[\frac{\mathbf{q} \cdot (\mathbf{k}+\mathbf{k}')}{|\mathbf{k}+\mathbf{k}'|}\right]^2 + \left[\frac{\mathbf{q} \cdot (\mathbf{k}-\mathbf{k}')}{|\mathbf{k}-\mathbf{k}'|}\right]^2\right\}, \quad (17)$$

which looks structurally similar to the response function of the electron gas with Coulomb interaction [26,27]. In evaluating Eq. (17) we generalize the analytic derivation presented in Ref. [27] (see Appendix A for details). The additional term in Eq. (16) simply amounts to the square of the Lindhard function χ_0, so that Eq. (16) reads as $f(q) = I(q) - \frac{\pi}{3}\chi_0^2(q)$. In the zero temperature limit we obtain for $f(q)$ the following expression:

$$f(q) = \frac{m_e^2 k_F^2}{16\pi^3\hbar^4 q^2} \left\{ \frac{2}{45q}(7q^5 - 15q^4 + 30q^3 - 20q^2 - 144)\ln|a| + \frac{2}{45q}(7q^5 + 15q^4 + 30q^3 + 20q^2 + 144)\ln b \right.$$

$$+ \frac{4}{45}q^2(7q^2 + 60)\ln\frac{2}{q} + \frac{16}{45}(11q^2 - 18) - \frac{2}{3}q\left[(2b)^3\ln b\left(\ln b + \ln\frac{2}{q}\right) - (2a)^3\ln|a|\left(\ln|a| + \ln\frac{2}{q}\right)\right]$$

$$\left. + 8\int_{-a}^b dz\, z\ln|z|[(a+z)(b-z)W_1(z) - (b+z)(z-a)W_2(z)] - \frac{4}{3}\left(q + ab\ln\left|\frac{b}{a}\right|\right)^2\right\}, \quad (18)$$

where $W_1(z) = \ln|\frac{z+a}{z-b}|$ and $W_2(z) = \ln|\frac{z-a}{z+b}|$, with $a = 1 - q/2$ and $b = 1 + q/2$ in units of the Fermi vector k_F.

The remaining self-energy diagrams (b) and (c) of Fig. 2 give a null contribution to the dipolar x energy (as it can be easily checked by evaluating the trace over the spin indices). The physical explanation for this result is that diagram (a), including two triplet Green's functions, correspond to the Fock (x) energy diagram for a magnetic HEG, whereas both diagrams (b) and (c) contain one singlet Green's function [28].

For completeness we show here the expansions of $f(q)$ at small and large q:

$$f(q) = \begin{cases} \frac{m_e^2 k_F^2}{1080\pi^3\hbar^4}\left[\frac{(127 + 60\log 2 - 60\log q)q^2}{5} - \frac{97q^4}{70} - \frac{53q^6}{392} + \dots\right], & q \to 0 \\ \frac{16 m_e^2 k_F^2}{675\pi^3\hbar^4}\left(\frac{25}{q^4} + \frac{11}{q^6} + \dots\right), & q \to \infty. \end{cases} \quad (19)$$

From Eq. (19) we observe that the second derivative of the functional has a logarithmic divergence in the low wave-vector limit $q = 0$. This nonanalyticity implies the nonexistence of standard semilocal gradient approximations and can be traced back to the nonlocal character of the interaction.

In Fig. 3 we show the function $f(q)$ and the x kernel $K_x^{zz}(q)$ computed from Eq. (12) at $r_s = 1$. At large q, $K_x^{zz}(q)$ tends to a constant value. In this limit the dipolar x energy amounts to one quarter of the magnetostatic energy. In Figs. 3(b)–3(d) we compare the Fourier transform of $K_x^{zz}(q)$ (see Appendix C)

to the interaction between classical magnetic dipoles, $4\pi d_{zz}$, for different values of the charge density. In the short-distance limit ($R \to 0$) both $K_x^{zz}(R)$ and the classical dipole interaction increase as $1/R^3$ [Fig. 3(b)]. At distances of few atomic units the x kernel decays, faster at higher charge density, while developing an oscillatory behavior [Fig. 3(c)]. The oscillations are readily seen in the ratio between $K_x^{zz}(R)$ and $4\pi d_{zz}$ [Fig. 3(d)], with a period that depends strongly on the value of the density. At high density ($r_s = 1$) the oscillations are fast, with a period of few atomic units, whereas at low density
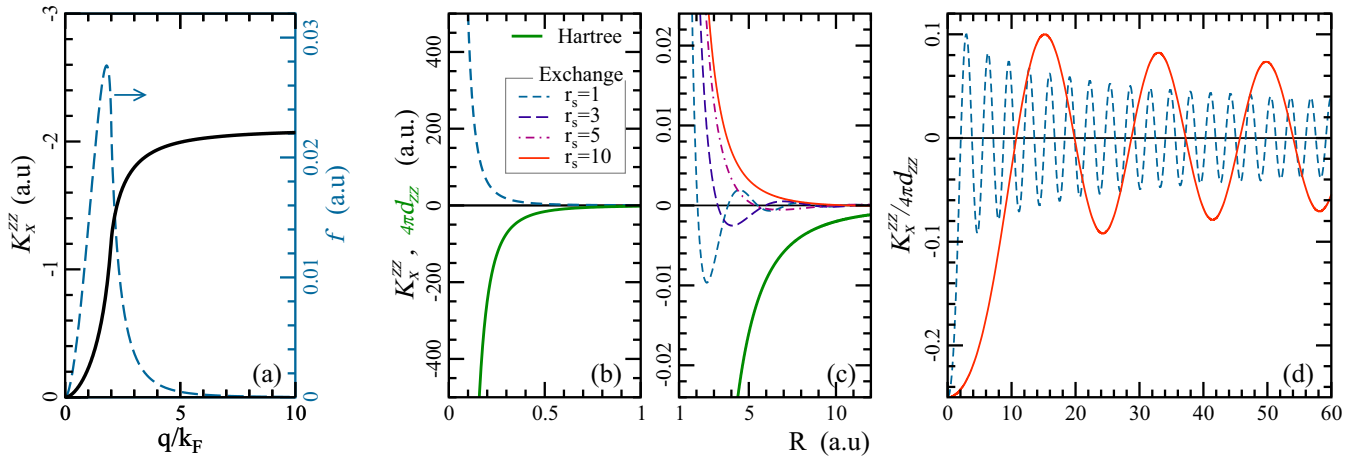
FIG. 3. Real and reciprocal space behavior of the dipolar exchange kernel. **q** and **R** are taken along the **z** axis; q is measured in units of the Fermi vector k_F, R is given in atomic units (Bohr). (a) Dipolar exchange kernel $K_x^{zz}(q)$ (black line) and energy functional $f(q)$ (dashed line) at $r_s = 1$. (b) Short-distance $K_x^{zz}(R)$ at $r_s = 1$ (short-dashed line) compared to the Hartree (magnetostatic) contribution (green line). (c) Mid-distance $K_x^{zz}(R)$ at $r_s = 1$ (short-dashed line), 3 (long-dashed line), 5 (dot-dashed line), and 10 (red line) compared to the Hartree (magnetostatic) contribution (green line). (d) Ratio between dipolar exchange and Hartree at $r_s = 1$ (dashed line) and $r_s = 10$ (red line).

($r_s = 10$) they lie in the long period range and eventually disappear in the limit $r_s \to \infty$. The oscillation amplitude (of the ratio) decreases slowly with R and, for realistic values of r_s, remains sizable ($\approx 5\%$) even at large interatomic distances. We expect that in conventional magnets, with mostly simple magnetic patterns and domain wall geometries, these oscillatory corrections to the magnetostatic energy will average to zero, especially in the high density limit. However, in more complex magnetic configurations, such as layered and frustrated systems [8,29,30], the oscillatory x energy may sum up leading to sizable and measurable effects.

III. SPIN-SPIN CONTACT FUNCTIONAL

As mentioned in Sec. I, in addition to the dipolar term, the magnetic interaction between two electrons includes also a spin-spin contact term [Eq. (5)]. This contact interaction has the same form of the Coulomb exchange interaction but is rescaled by the smaller factor μ_B^2. The associated Hartree functional is easily obtained as

$$E_H^{SC} = -\frac{4\pi \mu_B^2}{3} \int d^3r \, \mathbf{m}^2(\mathbf{r}), \tag{20}$$

while the LSDA for the x energy is given by

$$E_x^{SC} = 2\pi \mu_B^2 \int d^3r \left[n^2(\mathbf{r}) - \frac{1}{3}\mathbf{m}^2(\mathbf{r}) \right], \tag{21}$$

where n is the total electron density.

IV. CONCLUSIONS

We have proposed a density functional treatment of the dipolar interaction between electronic spin magnetic moments. Within this approach, the dipolar Hartree term is given by the classical magnetostatic energy, currently implemented in magnetic structure codes. In addition, we have derived quantum corrections by evaluating analytically the exact x energy (Fock term) for the magnetic electron gas with spin-spin interactions. The dipolar x energy thereby obtained amounts to one quarter of the magnetostatic energy at short interaction distance, or in the limit of low electronic density. At long range, the dipolar x kernel displays an oscillatory behavior, while decaying in amplitude slightly faster than the classical contribution [see Fig. 3(d)]. This quantum correction is expected to have negligible effects in most conventional magnetic materials, where it likely averages to zero. However, it might become significant in complex magnetic structures, especially in specific geometries where lattice and dipole x oscillations are commensurate, or in the presence of a delicate magnetic balance, like in frustrated systems. Further progress in the functional approximation might be achieved by carrying out the Levy constrained search [31,32] for the exact functional

$$F[n, \mathbf{m}]$$
$$= \min_{\Psi \to n, \mathbf{m}} \left\langle \Psi \left| \hat{T} + \frac{e^2}{2} \int d^3r \int d^3r' \frac{\hat{n}(\mathbf{r})\hat{n}(\mathbf{r}')}{|\mathbf{r} - \mathbf{r}'|} + \hat{H}^{SS} \right| \Psi \right\rangle, \tag{22}$$

via a stochastic minimization [33] over the many-body wave functions Ψ that are eigenstates of the total (spin+orbital) angular momentum $\hat{\mathbf{J}}^2$. Upcoming work comprises implementing and testing the new functional against experimental data. Applications include the study of crystalline layered magnets and magnetic atoms on surfaces, as well as the dynamics of domain walls and skyrmions. Of particular interest is also the application of our functional to the physics of dipolar quantum gases, where it might serve as an exchange partner for the "strictly correlated particles" functional of Ref. [34].

APPENDIX A: EVALUATION OF $I(q)$

For convenience we evaluate Eq. (17) in cylindrical coordinates with the polar axis along **q**, where all the wave vectors are measured in units of k_F. The integrations over the azimuthal and radial coordinates of **k** and **k'** are readily carried through obtaining

$$I(q) = \frac{m_e^2 k_F^2}{16\pi^3 \hbar^4 q^2} \sum_{i=0}^{3} J_i, \tag{A1}$$

where

$$J_0 = -2 \iint_{-a}^{b} \frac{dz\, dz'}{z\, z'} [(z^2 + z'^2)(\lambda + \lambda')(2\ln 2 + 1) + z^4 + 6z^2 z'^2 + z'^4], \tag{A2}$$

$$J_1 = 2 \iint_{-a}^{b} \frac{dz\, dz'}{z\, z'} [\alpha^2 \sqrt{R(z, z')} + \beta^2 |\beta|], \tag{A3}$$

$$J_2 = 4 \iint_{-a}^{b} \frac{dz\, dz'}{z\, z'} \lambda [\alpha^2 \ln |2\sqrt{R(z, z')} + \lambda' - \lambda + \alpha^2| + \beta^2 \ln |2|\beta| + \lambda' - \lambda + \beta^2|], \tag{A4}$$

$$J_3 = -4 \iint_{-a}^{b} \frac{dz\, dz'}{z\, z'} \lambda [\beta^2 \ln |\beta^2| + \alpha^2 \ln |\alpha^2|]. \tag{A5}$$

We adopt the same notation as in Ref. [27]. Here, $a = 1 - q/2$, $b = 1 + q/2$, $\alpha = z + z'$, $\beta = z - z'$, and $\lambda^{(')} = (a + z^{(')})(b - z^{(')})$. The function R is defined as $R(z, z') = C_0(z)z'^2 + B_0(z)z' + A_0(z)$, where $A_0 = z^2$, $B_0 = (2 + 2qz - q^2)z$, and $C_0 = 1 + 2qz$. Evaluating J_0 is straightforward and the resulting expression is

$$J_0 = -(2 + \ln 2)8q^2 - 2q \left[q^2 \ln 2 - \frac{4}{3}(4 + 5\ln 2) \right] \ln \left| \frac{a}{b} \right|. \tag{A6}$$

J_1 can be rewritten in the following form

$$J_1 = 4 \iint_{-a}^{b} dz\, dz' \left(\frac{\alpha}{z'} \sqrt{R(z, z')} + \frac{\beta}{z'} |\beta| \right) = 4 \int_{-a}^{b} dz (\bar{J}_1^A(z) + \bar{J}_1^B(z)), \tag{A7}$$

where $\bar{J}_1^A(z)$ and $\bar{J}_1^B(z)$ are evaluated to be [27]

$$\bar{J}_1^A(z) = 1 + \frac{1}{4}q^2 + \frac{5}{2}qz + \left(2 - \ln \left| 1 - \frac{4}{q^2} \right| \right) z^2 + \frac{B_0}{4C_0}(2z + q) + \frac{1}{4C_0^{3/2}} z^2 [8 - q^4 + 4qz(6 - q^2) + 12q^2 z^2] Y(z),$$

$$\bar{J}_1^B(z) = 2qz - 1 - \frac{q^2}{4} - z^2 (3 - 2\ln|z| + \ln|ab|),$$

with $Y(z) = \ln |\frac{\sqrt{C_0} + 1}{\sqrt{C_0} - 1}|$. The remaining integration in Eq. (A7) can also be carried through obtaining

$$J_1 = -\frac{1}{q^2} - \frac{1}{9} + \frac{44}{3}q^2 + 4\left(\frac{4}{3} + q^2 \right) \ln \frac{q}{2} + \frac{1}{3}[(q - 2)^3 \ln b - (q + 2)^3 \ln |a|] + \frac{1}{2q^3}(q^2 - 1)^2 \ln \left| \frac{q + 1}{q - 1} \right|$$

$$+ \frac{3}{4q^3} \eta_5 - \frac{1}{2q} \eta_3 - \left(\frac{5}{2q^3} - \frac{3}{2q} + \frac{q}{4} \right) \eta_1 - \left(\frac{3}{2q} - \frac{2}{q^3} - \frac{q}{2} \right) \eta_{-1} + \left(\frac{1}{2q} - \frac{1}{4q^3} - \frac{q}{4} \right) \eta_{-3}, \tag{A8}$$

where $\eta_n = q \int_{-a}^{b} dz\, C_0^{n/2} Y(z)$. The explicit expressions for $\eta_{\pm 1, -3}$ are given in Ref. [27], for $\eta_{3,5}$ in Appendix B.

Next, we evaluate $J_{23} = J_2 + J_3$. This term is conveniently rewritten as

$$J_{23} = 4 \iint_{-a}^{b} dz\, dz' \frac{\lambda}{z\, z'} (\alpha^2 + \beta^2) \ln |4\lambda| - 4 \int_{-a}^{b} dz \frac{\lambda}{z} [\bar{N}_1(z) + \bar{N}_2(z)], \tag{A9}$$

where $\bar{N}_1(z)$ and $\bar{N}_2(z)$ are defined as follows:

$$\bar{N}_1(z) = \int_{-a}^{b} dz' \frac{\alpha^2}{z'} \ln |\alpha^2 + \lambda' - \lambda - 2\sqrt{R(z, z')}|, \tag{A10}$$

$$\bar{N}_2(z) = \int_{-a}^{z} dz' \frac{\beta^2}{z'} \ln |2\beta(z - b)| + \int_{z}^{b} dz' \frac{\beta^2}{z'} \ln |2\beta(z + a)|. \tag{A11}$$

Equations (A10) and (A11) can be integrated by parts obtaining

$$\bar{N}_1(z) = \int_{-a}^{b} \frac{dz'}{\alpha} \left(z^2 \ln|z'| + \frac{1}{2}z'^2 + 2zz' \right) \left(\frac{qz}{\sqrt{R(z, z')}} - 1 \right) + \left(z^2 \ln \left| \frac{b}{a} \right| + q + 4z \right) \ln |2\lambda| \tag{A12}$$

$$\bar{N}_2(z) = \left(z^2 \ln \left| \frac{b}{a} \right| + q - 4z \right) \ln |2\lambda| + \left(\frac{3}{2}z^2 - \ln |z|z^2 \right) W_1(z) + \int_{-a}^{b} dz' \left(z^2 \ln|z'| + \frac{1}{2}z'^2 - 2zz' \right) \frac{1}{\beta}, \tag{A13}$$

where we have used the notation $W_1(z) = \ln|\frac{z+a}{z-b}|$. Subsequent substitution of Eqs. (A12) and (A13) in Eq. (A9) gives

$$J_{23} = 4q\left[q + \left(ab + \frac{2}{3}\right)\ln\left|\frac{b}{a}\right|\right](2\ln 2 + 1) - \frac{8}{3}q\ln\left|\frac{b}{a}\right| + 6\int_{-a}^{b}dz\lambda zW_2(z) - 4(q\Phi_1 + 2\Phi_2 + q\Phi_3 - \Phi_4). \tag{A14}$$

Here, we have defined $W_2(z) = \ln|\frac{z-a}{z+b}|$,

$$\Phi_1 = \int_{-a}^{b}dz\lambda\int_{-a}^{b}dz'\left(\frac{1}{2}z'^2 + 2zz'\right)\frac{1}{\alpha\sqrt{R(z,z')}}, \tag{A15}$$

$$\Phi_2 = \int_{-a}^{b}dz\lambda z\int_{-a}^{b}dz'\frac{z'}{\alpha\beta}\ln|z'|, \tag{A16}$$

$$\Phi_3 = \int_{-a}^{b}dz\lambda\int_{-a}^{b}dz'z^2\ln|z'|\frac{1}{\alpha\sqrt{R(z,z')}}, \tag{A17}$$

$$\Phi_4 = \int_{-a}^{b}dz\lambda zW_1(z)\ln|z|. \tag{A18}$$

By writing Φ_1 as

$$\Phi_1 = \frac{1}{2}\int_{-a}^{b}dz\lambda\int_{-a}^{b}dz'\frac{1}{\sqrt{R(z,z')}}\left[z' + 3z\left(1 - \frac{z}{\alpha}\right)\right], \tag{A19}$$

and performing the integrations over z'

$$\int_{-a}^{b}dz'\frac{z'}{\sqrt{R(z,z')}} = \frac{1}{C_0}(2z + q) - \frac{B_0}{C_0^{3/2}}Y(z), \tag{A20}$$

$$\int_{-a}^{b}dz'\frac{1}{\sqrt{R(z,z')}} = \frac{2}{\sqrt{C_0}}Y(z), \tag{A21}$$

$$\int_{-a}^{b}dz'\frac{1}{\alpha\sqrt{R(z,z')}} = -\frac{1}{qz}W_2(z), \tag{A22}$$

we get

$$\Phi_1 = \frac{1}{2}\int_{-a}^{b}dz\frac{\lambda}{\sqrt{C_0}}\left[\frac{2z+q}{\sqrt{C_0}} + \left(6z - \frac{B_0}{C_0}\right)Y(z)\right] + \frac{3}{2q}\int_{-a}^{b}dz\lambda zW_2(z). \tag{A23}$$

The last term in Eq. (A23) cancels with the same contribution of opposite sign in Eq. (A14). The remaining integrals can be carried out as follows

$$\frac{1}{2}\int_{-a}^{b}dz\lambda\frac{2z+q}{C_0} = \frac{1}{24q^4}\left[-6q + 16q^3 + 6q^5 - 3(q^2 - 1)^3\ln\left|\frac{q+1}{q-1}\right|\right], \tag{A24}$$

$$-\frac{1}{2}\int_{-a}^{b}dz\lambda\frac{Y(z)}{C_0^{3/2}}[B_0 - 6zC_0] = -\frac{5}{16q^4}\eta_5 + \left(\frac{9}{16q^2} + \frac{1}{q^4}\right)\eta_3 - \left(\frac{3}{16} - \frac{1}{16q^2} + \frac{9}{8q^4}\right)\eta_1$$

$$- \left(\frac{q^2}{16} - \frac{3}{8} + \frac{13}{16q^2} - \frac{1}{2q^4}\right)\eta_{-1} + \left(\frac{3}{16q^2} - \frac{1}{16q^4} - \frac{3}{16} + \frac{q^2}{16}\right)\eta_{-3}. \tag{A25}$$

We then write Eq. (A16) as

$$\Phi_2 \overset{z \leftrightarrow z'}{=} -\int_{-a}^{b}dz z\ln|z|\int_{-a}^{b}dz'\frac{\lambda'z'}{\alpha\beta} \tag{A26}$$

$$= -\int_{-a}^{b}dz z\ln|z|\left[(b+z)(a-z)\int_{-a}^{b}dz'\frac{z'}{\alpha\beta} + (q+z)\int_{-a}^{b}dz'\frac{z'}{\beta} - \int_{-a}^{b}dz'\frac{z'^2}{\beta}\right], \tag{A27}$$

where each of the integrations in z' can be performed

$$\int_{-a}^{b}dz'\frac{z'}{\alpha\beta} = \frac{1}{2}(W_1(z) + W_2(z)), \tag{A28}$$

$$\int_{-a}^{b}dz'\frac{z'}{\beta} = -2 + zW_1(z), \tag{A29}$$

$$\int_{-a}^{b}dz'\frac{z'^2}{\beta} = \frac{1}{2}[a(a-2z) - b(b+2z)] + z^2W_1(z). \tag{A30}$$

Substituting Eqs. (A28)–(A30) in Eq. (A27), and carrying through the elementary integrations over z, we obtain the following result for Φ_2 in terms of one quadrature

$$\Phi_2 = -\frac{1}{2}\int_{-a}^{b} dz\, z[\lambda W_1(z) - (b+z)(z-a)W_2(z)]\ln|z| - \frac{1}{2}q(q + a^2\ln|a| - b^2\ln|b|). \tag{A31}$$

We follow the same procedure for Φ_3 given in Eq. (A17)

$$\Phi_3 \overset{z \leftrightarrow z'}{=} \int_{-a}^{b} dz\,\ln|z| \int_{-a}^{b} dz'\, \frac{\lambda' z'^2}{\alpha\sqrt{R(z,z')}}$$

$$= \int_{-a}^{b} dz\,\ln|z|\left[(b+z)(a-z)\int_{-a}^{b} dz'\, \frac{z'^2}{\alpha\sqrt{R(z,z')}} + (q+z)\int_{-a}^{b} dz'\, \frac{z'^2}{\sqrt{R(z,z')}} - \int_{-a}^{b} dz'\, \frac{z'^3}{\sqrt{R(z,z')}} \right]. \tag{A32}$$

Here, we have

$$\int_{-a}^{b} dz'\, \frac{z'^2}{\alpha\sqrt{R(z,z')}} = \frac{1}{C_0}(2z+q) - \frac{1}{C_0^{3/2}}(B_0 + 2zC_0)Y(z) - \frac{z}{q}W_2(z), \tag{A33}$$

$$\int_{-a}^{b} dz'\, \frac{z'^2}{\sqrt{R(z,z')}} = \left(\frac{b}{2C_0} - \frac{3B_0}{4C_0^2}\right)\sqrt{R(z,b)} + \left(\frac{a}{2C_0} + \frac{3B_0}{4C_0^2}\right)\sqrt{R(z,-a)} + \frac{2}{\sqrt{C_0}}\left(\frac{3B_0^2}{8C_0^2} - \frac{A_0}{2C_0}\right)Y(z), \tag{A34}$$

$$\int_{-a}^{b} dz'\, \frac{z'^3}{\sqrt{R(z,z')}} = \left(\frac{b^2}{3C_0} - \frac{5B_0 b}{12C_0^2} + \frac{5B_0^2}{8C_0^3} - \frac{2A_0}{3C_0^2}\right)\sqrt{R(z,b)} - \left(\frac{a^2}{3C_0} + \frac{5B_0 a}{12C_0^2} + \frac{5B_0^2}{8C_0^3} - \frac{2A_0}{3C_0^2}\right)\sqrt{R(z,-a)}$$

$$- \left(\frac{5B_0^3}{16C_0^3} - \frac{3A_0 B_0}{4C_0^2}\right)\frac{2}{\sqrt{C_0}}Y(z). \tag{A35}$$

Substituting Eqs. (A33)–(A35) in Eq. (A32), we obtain with some algebra

$$\Phi_3 = \bar{\Phi}_1 + \bar{\Phi}_2 + \bar{\Phi}_3, \tag{A36}$$

where

$$\bar{\Phi}_1 = -\frac{1}{q}\int_{-a}^{b} dz\, z\ln|z|(b+z)(a-z)W_2(z), \tag{A37}$$

$$\bar{\Phi}_2 = \int_{-a}^{b} dz\left[-\frac{19}{32q^3}C_0^2 + \left(\frac{139}{96q^3} - \frac{9}{32q}\right)C_0 - \frac{15}{16q^3} + \frac{25}{16q} - \frac{5}{32}q + \left(\frac{1}{16q^3} - \frac{3}{4q} + \frac{17}{32}q + \frac{q^3}{32}\right)C_0^{-1} \right.$$

$$\left. + \left(-\frac{1}{16q} - \frac{13}{96q^3} + \frac{5q}{32} + \frac{q^3}{24}\right)C_0^{-2} + \left(\frac{5}{32q^3} - \frac{15}{32q} + \frac{15}{32}q - \frac{5}{32}q^3\right)C_0^{-3}\right]\ln|z|, \tag{A38}$$

$$\bar{\Phi}_3 = \int_{-a}^{b} dz\, C_0^{-7/2}\left[\left(-4 + 2q^2 - \frac{q^4}{4}\right)z + \left(-16 + \frac{11}{2}q^3 - \frac{q^5}{4}\right)z^2 + \left(8 - 20q^2 + \frac{11}{2}q^4 - \frac{q^6}{8}\right)z^3 \right.$$

$$\left. + \left(36q + 2q^3 + \frac{5}{4}q^5\right)z^4 + \left(60q^2 + \frac{25}{2}q^4\right)z^5 + 35q^3 z^6\right]\ln|z|Y(z). \tag{A39}$$

Evaluating $\bar{\Phi}_2$ is elementary. Moreover, it can be shown [27] that $\bar{\Phi}_3$ is equivalent to

$$\bar{\Phi}_3 = \frac{1}{8q}\sum_{n=-3}^{3}\gamma_n\frac{1}{2n+1}\left[(1+q)^{2n+1}\ln b\ln\left|\frac{2b}{q}\right| - \tilde{q}^{2n+1}\ln|a|\ln\left|\frac{\tilde{q}+1}{\tilde{q}-1}\right| + \Omega_n\right], \tag{A40}$$

where

$$\gamma_3 = \frac{35}{8q^3},\ \gamma_2 = -\frac{45}{4q^3} + \frac{25}{8q},\ \gamma_1 = \frac{69}{8q^3} - \frac{117}{8q} + \frac{5}{8}q,\ \gamma_0 = -\frac{3}{2q^3} + \frac{29}{4q} + 3q - \frac{q^3}{8},$$

$$\gamma_{-1} = -\frac{3}{8q^3} + \frac{11}{4q} - \frac{7}{4}q - \frac{q^3}{8},\ \gamma_{-2} = \frac{3}{4q^3} - \frac{3}{8q} - \frac{3q^3}{8},\ \gamma_{-3} = -\frac{5}{8q^3} + \frac{15}{8q} - \frac{15}{8}q + \frac{5q^3}{8}.$$

Here, $\tilde{q} = |1-q|$ and the explicit expressions for $\Omega_{0,\pm 1}$ are given in Ref. [27], while for $\Omega_{\pm 2,\pm 3}$ in Appendix B.

APPENDIX B

$$\eta_3 = \tfrac{1}{5}[4q(2+q^2) - 2q(5 + 10q^2 + q^4)\ln q - 2(1 - 2q + 4q^2 - 3q^3 + q^4)a\ln|2a| + 2(1 + 2q + 4q^2 + 3q^3 + q^4)b\ln 2b], \tag{B1}$$

$$\eta_5 = \frac{1}{7}\left[4q\left(3 + \frac{13}{3}q^2 + q^4\right) - 2q(7 + 35q^2 + 21q^4 + q^6)\ln q - 2(1 - 3q + 9q^2 - 13q^3 + 11q^4 - 5q^5 + q^6)a\ln|2a|\right.$$

$$\left. + 2(1 + 3q + 9q^2 + 13q^3 + 11q^4 + 5q^5 + q^6)b\ln 2b\right], \tag{B2}$$

$$\eta_{-5} = \frac{1}{3}\left[\frac{4q}{(q^2-1)^2} + 2\ln\left|\frac{q+1}{q-1}\right| - \left(1 + \frac{1}{(1+q)^3}\right)\ln 2b + \left(1 + \frac{1}{(1-q)^3}\right)\ln|2a| + \frac{2q(q^2+3)}{(q^2-1)^3}\ln q\right]. \tag{B3}$$

$$\Omega_{-3} = h_0(q) - 2q\left[\int_{-a}^{b} dz\left(C_0^{-3} + C_0^{-2} + C_0^{-1}\right)\ln|z|\right] + 2(\eta_{-3} + \eta_{-5}), \tag{B4}$$

where $h_0(q)$ is given in Ref. [27],

$$\Omega_{-2} = h_0(q) - 2q\left[\int_{-a}^{b} dz\left(C_0^{-2} + C_0^{-1}\right)\ln|z|\right] + 2\eta_{-3}, \tag{B5}$$

$$\Omega_2 = h_0(q) - \frac{1}{30}[q(416 + 108q^2) + q(240 + 120q^2)\ln 2 - q(60 + 300q + 80q^2 + 75q^3 + 12q^4)\ln q$$

$$+ (2b)(92 - 16q + 38q^2 + 21q^3 + 12q^4)\ln 2b - (\tilde{q} + 1)(137 - 77\tilde{q} + 47\tilde{q}^2 - 27\tilde{q}^3 + 12\tilde{q}^4)\ln|\tilde{q} + 1|$$

$$+ (\tilde{q} - 1)(137 + 77\tilde{q} + 47\tilde{q}^2 + 27\tilde{q}^3 + 12\tilde{q}^4)\ln|\tilde{q} - 1|], \tag{B6}$$

$$\Omega_3 = h_0(q) + \frac{1}{210}\left[-q\left(4472 + \frac{9028}{3}q^2 + 520q^4\right) - q(2520 + 3640q^2 + 840q^4)\ln 2 + q(420 + 4410q + 1260q^2\right.$$

$$+ 3675q^3 + 924q^4 + 490q^5 + 60q^6)\ln q - 2b(704 - 142q + 386q^2 + 437q^3 + 464q^4 + 230q^5 + 60q^6)\ln 2b$$

$$+ (\tilde{q} + 1)(1089 - 669\tilde{q} + 459\tilde{q}^2 - 319\tilde{q}^3 + 214\tilde{q}^4 - 130\tilde{q}^5 + 60\tilde{q}^6)\ln|\tilde{q} + 1| - (\tilde{q} - 1)(1089 + 669\tilde{q}$$

$$+ 459\tilde{q}^2 + 319\tilde{q}^3 + 214\tilde{q}^4 + 130\tilde{q}^5 + 60\tilde{q}^6)\ln|\tilde{q} - 1|. \tag{B7}$$

APPENDIX C: FOURIER TRANSFORM OF $K_x^{ij}(\mathbf{q})$

The real-space representation of Eq. (11) is given by

$$E_x^{\mathrm{dip}}[\mathbf{m}] = \frac{\mu_B^2}{2}\int d^3r\, d^3r'\, K_x^{ij}(\mathbf{R})\delta\mathbf{m}_i(\mathbf{r})\delta\mathbf{m}_j(\mathbf{r}'), \tag{C1}$$

where

$$K_x^{ij}(\mathbf{R}) = \frac{g_{kl}(\mathbf{R})}{\chi_0^{ik}(R)\chi_0^{jl}(R)}. \tag{C2}$$

Here, $g_{kl}(\mathbf{R})$ is evaluated as follows. We write the Fourier transform of $g_{kl}(\mathbf{q})$ in spherical coordinates as:

$$g_{kl}(\mathbf{R}) = \frac{1}{(2\pi)^3}\int_{-\infty}^{\infty} g_{kl}(\mathbf{q})e^{i\mathbf{q}\cdot\mathbf{R}}d^3q = \frac{1}{(2\pi)^3}\int_0^{\infty} dq\int_0^{2\pi} d\phi\int_{-\frac{\pi}{2}}^{\frac{\pi}{2}} d\theta\, f(q)2P_2(\cos\theta)e^{i\mathbf{q}\cdot\mathbf{R}}q^2\sin\theta. \tag{C3}$$

Then, by expressing the exponential as a Rayleigh expansion, and using the addition theorem for spherical harmonics $Y_{lm}(\theta, \phi)$, we obtain:

$$g_{kl}(\mathbf{R}) = \frac{2}{(2\pi)^2}\int_0^{2\pi}\int_{-\frac{\pi}{2}}^{\frac{\pi}{2}}\sum_{l=0}^{\infty}\sum_{m=-l}^{l} Y_{20}(\theta, \phi)Y_{lm}(\theta, \phi)\sin\theta d\phi d\theta\int_0^{\infty} f(q)i^l j_l(qR)q^2 dq\, 2P_2(\cos\theta_{\mathbf{R}}) \tag{C4}$$

$$= -\frac{2}{(2\pi)^2}\int_0^{\infty} f(q)j_2(qR)q^2 dq\, 2P_2(\cos\theta_{\mathbf{R}}) = f(R)2P_2(\cos\theta_{\mathbf{R}}), \tag{C5}$$

where $j_l(qR)$ are the spherical Bessel functions and the function $f(R)$ is defined by the last equality.

[1] A. Steane, Rep. Prog. Phys. **61**, 117 (1998).

[2] L. You and M. S. Chapman, Phys. Rev. A **62**, 052302 (2000).

[3] S. Ghosh, T. F. Rosenbaum, G. Aeppli, and S. N. Coppersmith, Nature (London) **425**, 48 (2003).

[4] J. Tejada, E. M. Chudnovsky, E. del Barco, J. M. Hernandez, and T. P. Spiller, Nanotechnology **12**, 181 (2001).

[5] C. Tannous and R. L. Comstock, Magnetic information-storage materials, in *Springer Handbook of Electronic and Photonic*

Materials, edited by S. Kasap and P. Capper (Springer International Publishing, Cham, 2017), pp. 1–1.

[6] M. Lu, N. Q. Burdick, S. H. Youn, and B. L. Lev, Phys. Rev. Lett. **107**, 190401 (2011).

[7] M. Lu, N. Q. Burdick, and B. L. Lev, Phys. Rev. Lett. **108**, 215301 (2012).

[8] B. C. den Hertog and M. J. P. Gingras, Phys. Rev. Lett. **84**, 3430 (2000).

[9] A. Fernández-Pacheco, R. Streubel, O. Fruchart, R. Hertel, P. Fischer, and R. P. Cowburn, Nat. Commun. **8**, 15756 (2017), review article .

[10] Y.-S. Ding, Y.-F. Deng, and Y.-Z. Zheng, Magnetochemistry **2**, 40 (2016).

[11] J. Fidler and T. Schrefl, J. Phys. D: Appl. Phys. **33**, R135 (2000).

[12] P. Hohenberg and W. Kohn, Phys. Rev. **136**, B864 (1964).

[13] R. M. Dreizler and E. Gross, *Density Functional Theory* (Springer-Verlag, Berlin Heidelberg, 1990).

[14] E. Engel and R. M. Dreizler, *Density Functional Theory- An Advanced Course* (Springer-Verlag, Berlin, 2011).

[15] U. von Barth and L. Hedin, J. Phys. C: Solid State Phys. **5**, 1629 (1972).

[16] W. Kohn and L. J. Sham, Phys. Rev. **140**, A1133 (1965).

[17] T. Itoh, Rev. Mod. Phys. **37**, 159 (1965).

[18] The quasirelativistic Hamiltonian for electrons contains an additional pairwise spin-dependent term, i.e., the spin-other orbit interaction. In the present work we focus on the treatment of spin-spin interactions.

[19] H. A. Bethe and E. E. Salpeter, *Quantum Mechanics of One- and Two-Electron Atoms* (Plenum/Rosetta, New York, 1977).

[20] A. Stewart, Sri Lankan J. Phys. **12**, 33 (2012).

[21] C. Cohen-Tannoudji, J. Dupont-Roc, and G. Grynberg, "Classical electrodynamics: The fundamental equations and the dynamical variables", in *Photons and Atoms* (Wiley, Weinheim, 2004), Chap. 1, pp. 5–77.

[22] H. J. F. Jansen, Phys. Rev. B **38**, 8022 (1988).

[23] P. S. Svendsen and U. Von Barth, Int. J. Quantum Chem. **56**, 351 (1995).

[24] P. S. Svendsen and U. von Barth, Phys. Rev. B **54**, 17402 (1996).

[25] E. Engel, Phys. Rev. A **51**, 1159 (1995).

[26] E. Engel and S. H. Vosko, Phys. Rev. B **42**, 4940 (1990).

[27] Z. Qian, J. Math. Phys. **56**, 111901 (2015).

[28] By triplet (singlet) Green's function we refer to the spin-vector (spin-scalar) component of the full spinor Green's function $G(12) = \frac{1}{2}\{g_n(12) + \sigma \cdot \mathbf{g_s}(12)\}$ [35].

[29] D. C. Johnston, Phys. Rev. B **93**, 014421 (2016).

[30] Y. Chen, A. Dahal, J. Rodriguez-Rivera, G. Xu, T. Heitmann, V. Dugaev, A. Ernst, and D. Singh, Materials Today Phys. **12**, 100163 (2019).

[31] M. Levy, Phys. Rev. A **26**, 1200 (1982).

[32] E. H. Lieb, *Physics as Natural Philosophy*, edited by A. Shimony and H. Feshbach (MIT Press, Cambridge, 1982), p. 111.

[33] P. Mori-Sánchez and A. J. Cohen, J. Phys. Chem. Lett. **9**, 4910 (2018).

[34] F. Malet, A. Mirtschink, C. B. Mendl, J. Bjerlin, E. O. Karabulut, S. M. Reimann, and P. Gori-Giorgi, Phys. Rev. Lett. **115**, 033006 (2015).

[35] A. K. Rajagopal and M. Mochena, Phys. Rev. B **62**, 15461 (2000).